

# Experimental Analysis of a Low Cost Lift and Drag Force Measurement System for Educational Sessions

Asutosh Boro

B.Tech National Institute of Technology Srinagar  
Indian Institute of Science, Bangalore 560012

\*\*\*

**Abstract** - A low cost Lift and Drag force measurement system was designed, fabricated and tested in wind tunnel to be used for basic practical lab sessions. It consists of a mechanical linkage system, piezo-resistive sensors and NACA Airfoil to test its performance. The system was tested at various velocities and angle of attacks and experimental coefficient of lift and drag were then compared with literature values to find the errors. A decent accuracy was deduced from the lift data and the considerable error in drag was due to concentration of drag forces across a narrow force range and sensor's fluctuations across that range. It was inferred that drag system will be as accurate as the lift system when the drag forces are large. So overall the composed system performs well at large force ranges. In addition, the lift system was indirectly used to measure the wind tunnel velocity and results were compared with accurate values from a differential manometer. Results were good with an error of -6.5%. So the system could likewise be utilized to measure wind tunnel's fluid velocity. Overall, the budget for the system was very low in contrast to other measurement systems and this system proved good enough to be used for force and velocity analysis in practical sessions for students. Further, the same design could be experimented with different sensors for better accuracy and cost reduction

**Key Words:** Piezo-resistive, Naca, Mechanical Linkage, Wind Tunnel, Airfoil

## 1. INTRODUCTION

Any atmospheric flying objects, ships and cars need to go through various CFD simulations and wind tunnel tests for better design and lift & drag force tests are some of the most important tests that it has to go through. Coefficient of Lift and Drag are two of the primary concerns of these tests. Furthermore, flow over immersed bodies is an important part of fluid mechanics and it has to be experimentally experienced and visualized by a student. So wind tunnel experiments become very important. However, wind tunnel testing is expensive. And only a few educational Institutions in India have wind turbines with an accurate force measurement. A six component force balance device can cost up to lakhs which could sometimes be twice as much as the wind tunnel's cost. This paper presents a simple low cost design for a force measurement system that can easily be fabricated and arranged inside a

wind- tunnel and used for educational learning with good accuracy. In addition, an indirect wind tunnel velocity measurement capability of the designed system was tested. NACA airfoil 4209 was chosen as the test subject to measure its performance and tests were done at various angles of attack and velocities 11m/s, 12m/s and 14m/s. The force and coefficient results obtained were compared with literature data from airfoil tools[1] to find the system's accuracy.

## 1.1 Methodology

The phenomenon of Lift and drag is very complex and is theorized for better understanding by potential flow and boundary layer theory which has good agreements with experimental results [2]. Overall the complex theories derives two simple equations for lift and drag forces:

$$\text{Lift force} = \frac{1}{2} \rho v^2 A_y C_L$$

$$\text{Drag force} = \frac{1}{2} \rho v^2 A_x C_D$$

Where  $v$  is the free stream air velocity,  $\rho$  is the air density and  $A_y$  is the projected area of the object as seen from parallel to fluid flow and  $A_x$  is the projected area of the object as seen from perpendicular to the fluid flow.  $C_D$  and  $C_L$  contains all the complex dependencies and they are generally determined experimentally [ 3].

## 2. Design Chosen

The main parts of the design are consists of the following parts:

- i. Mechanical Linkage
- ii. Pulleys And Supports
- iii. Piezo resistive Sensors
- iv. Airfoil
- v. Microcontroller circuit

## 2.1 Mechanical Linkage

Mechanical linkages are made of aluminum strips for its lightweight and considerable stiffness Strips  $S_1$  and  $S_2$  are joined by rivets such that they can rotate freely about

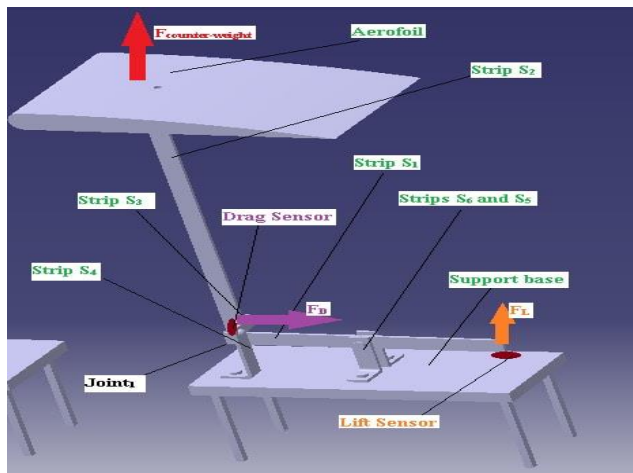


Figure 1. Mechanical Linkage System

joint<sub>1</sub>. The higher vertical end of S<sub>2</sub> is bolted to another strip S<sub>7</sub> which is bolted to the test subject such that angle of attack can be varied as shown in Figure 3. Strip S<sub>1</sub> is fixed with supporting strips S<sub>6</sub> and S<sub>5</sub> with nuts and bolts such that it can only rotate freely about its center of mass. Strips S<sub>5</sub> and S<sub>6</sub> are fixed with the supporting base as shown in Figure 1.

S<sub>3</sub> is fixed with S<sub>4</sub> and S<sub>4</sub> is fixed to the supporting base.

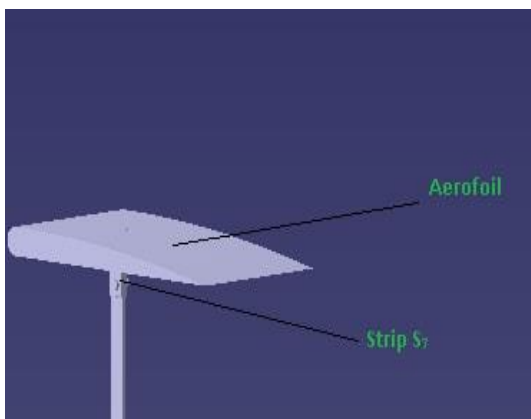


Figure 2. Airfoil with Strip S<sub>7</sub>

They are used to balance torque such that all the reaction force are exerted by the sensor. Linkage<sub>1</sub> consists of main strips S<sub>1</sub> and S<sub>2</sub>. Linkage<sub>1</sub> is used for lift force and Linkage<sub>2</sub> is used for drag force measurement. Linkage<sub>2</sub> consists of main strips S<sub>3</sub> and S<sub>4</sub>.

Since S<sub>1</sub> is fixed to rotate about its center of mass so if air tries to lift the foil with force F<sub>L</sub> this force will be transmitted by strip S<sub>2</sub> at joint<sub>1</sub> vertically and equal amount of force will be applied by any object kept at S<sub>1</sub>'s other end to maintain equilibrium. A force sensor will be kept at this location. S<sub>2</sub> can rotate about joint<sub>1</sub>. If air exerts a drag force F<sub>d</sub> on the foil, equilibrium can be maintained

by balancing torque by placing some resistance at a distance L<sub>1</sub> vertically above point<sub>1</sub> strip S<sub>3</sub> in this case. A sensor is placed at this resistance to measure the drag force

$$\text{Equilibrium equation: } F_D * L = F_s * L_1$$

$$F_D = F_s(L_1/L)$$

## 2.2 Pulleys and supports

For proper, easy reading and calibration, the self-weight of airfoil and linkage mechanism has to be continuously balanced otherwise the wind would have to first put a force equal to the weight of the foil to start showing sensor readings . A pulley system was designed as a solution as shown in Figure 3. The airfoil was hanged to the pulley and a counter weight was fixed to the other side of the pulley

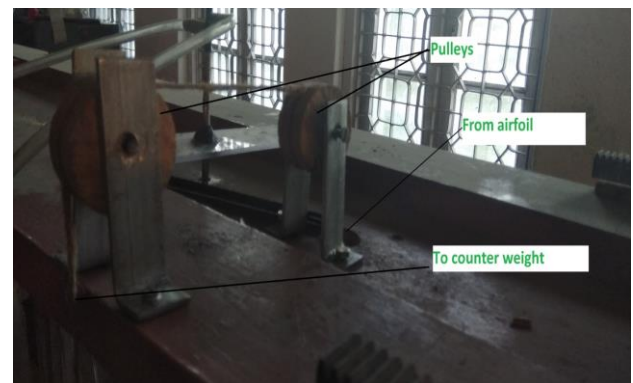


Figure 3. Pulley And Support System

Supporting desk is made of wood and its total weight is increased by adding sand bags so that total weight of the support remains greater than the maximum lift force the airfoil can encounter

## 2.3 Piezoresistive sensor



Figure 4. Piezo-resistive sensor [4]

Two flexi-force[4] piezo-resistive force sensors were used for drag and lift. These sensors are ideal for measuring force without disturbing the dynamics of tests. Both static and dynamic forces can be measured up to 100 lbf. They are thin enough to enable non-intrusive measurement. These sensors use a resistive based technology. The application of a force to the active sensing area of the sensor results in a change in the resistance of the sensing element in inverse proportion to the force applied. Piezo resistive sensors have ultra-thin and flexible printed circuit, which can be easily integrated into most applications. With its paper thin construction as shown in Figure 5, flexibility and force measurement ability, it can measure force between almost any two surfaces and is durable enough to stand up to most environments. It has better force sensing properties, linearity, hysteresis, drift and temperature sensitivity than any other thin-film force sensors. The active sensing area is a 0.375 diameter circle at the end of the sensor. So load should be evenly distributed throughout the circular sensing area for accurate sensing. Its calibration has been done with the provided resistance vs force relation as shown in Figure 5

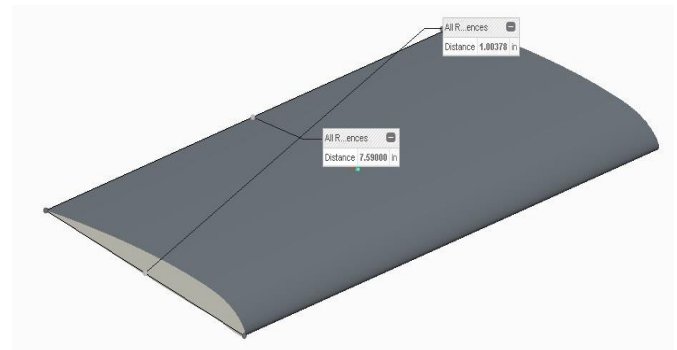


Figure 6. NACA 4209 Airfoil

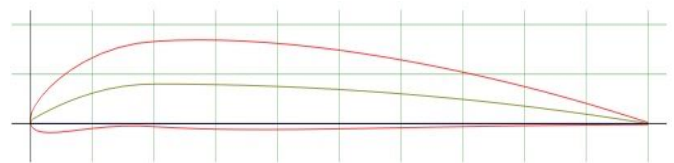


Figure 7. Line Diagram of NACA 4209 Airfoil

Chord length was taken as 39.5 cm  
 Maximum camber 4% of chord length  
 Maximum camber position at 20 % of chord length from leading edge  
 Maximum thickness 9% of chord length

**2.5 Microcontroller circuitry and coding**

Arduino[5] was used for its easy and fast prototyping. The circuitry is as shown in Figure 8

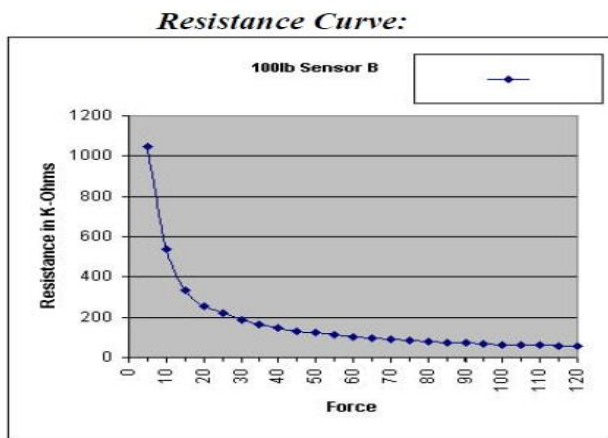


Figure 5. Resistance-Force Relation of sensor[4]

After analyzing the inverse relation between resistance and force one can approximately come to conclusion with the relation  $Force = (25304580/Resistance) N$ . This relation will be further used in program coding

**2.4 Airfoil**

NACA airfoil 4209 was chosen as the test subject as shown in Figure 6 and Figure 7. It was used because of its simplicity in design and fabrication. This type of airfoil is speed sensitive in that an increase in speed will causes your plane to climb. Flat bottom wings create a lot of lift and are very commonly seen in biplanes and high wing planes. These have a lot of drag. And these are very easy to control. Hence it was chosen since it will give better data. The experimental setup is as shown in Figure 9.

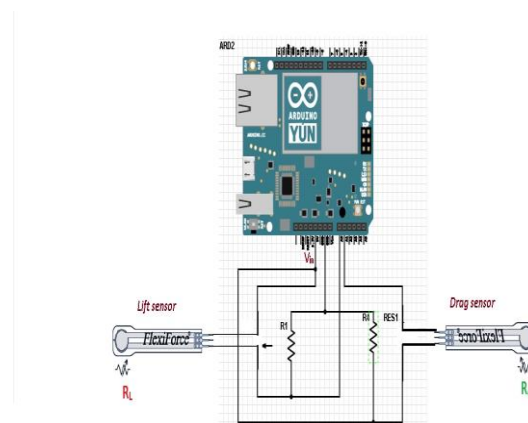


Figure 8. Arduino Board And Circuit

$R_1 = R_4 = 100000\text{ohms}$

Voltage in to both the sensors is 5 volts from Arduino . The system was tested at a constant voltage of 5 Volts. The sensitivity of the sensor can be increased by increasing the

voltage  
 $V_{in} = 5$  volts.

For Force and voltage relation has to be derived from the circuit:

For lift sensor:

$$V_{in} = I * (R_L + R_1)$$

$$V_{IN} - V_0 = I * R_L$$

$$V_0 = V_{in} [R_i / (R_L + R_i)]$$

Similarly for drag sensor:

$$V_1 = V_{in} [R_4 / (R_D + R_4)]$$

$V_0$  and  $V_1$  are analog inputs to Arduino by the lift sensor and drag sensor respectively, it further has to be converted to voltage. Arduino takes in input as analog data. It has to be converted to voltage to use it in voltage and force relation to get force readings. It has a linear voltage to analog relation (0-5v) to (0 - 1024) . Voltage = (5/1024)\*analog

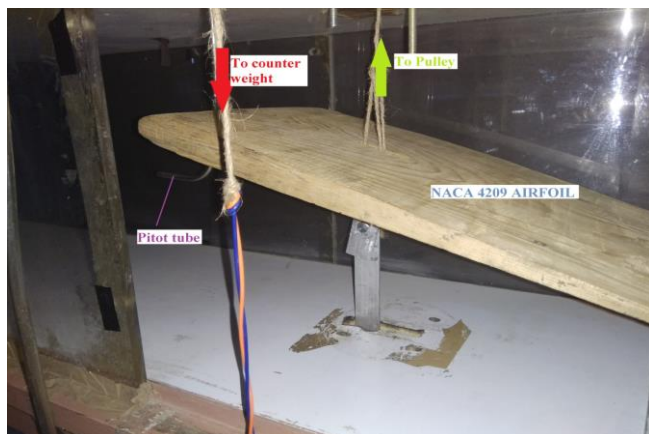


Figure 9. Airfoil setup

### 3. TESTING AND INVESTIGATION



Figure 10. Open Wind Tunnel

An open air wind tunnel was used as shown in Figure 10. Wind speed was checked against particular frequencies. Data for flow velocity was calculated with the help of differential manometer against corresponding frequency.

Table - 1: Frequency and flow velocity of wind tunnel

Motor Frequency( Hz)	Air Speed (m/s)
25	11
30	12
35	14
40	17
45	18
50	21
55	24

The pitot tube combined with a differential manometer works on the principle of subtracting the static pressure head from the stagnation pressure head provided the elevation is the same. The conversion takes place at the stagnation point, located at the pitot tube entrance. The pressure difference is measured by the differential manometer. The the equation for stagnation pressure becomes  $P_{stag} = P + 1/2 (\rho v^2)$ , which can be rearranged to  $V = (2 \Delta P / \rho)^{1/2}$ . Where  $\Delta P = P_{stag} - P$ .

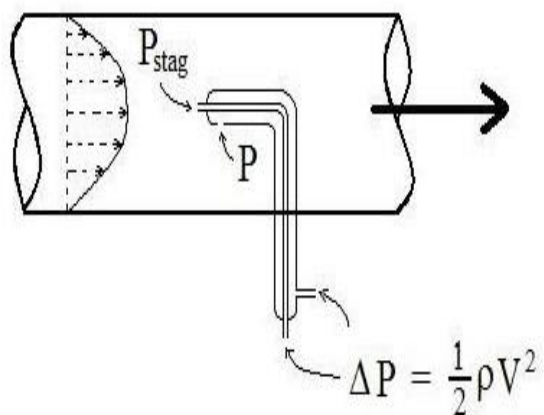


Figure 11. Pitot tube with velocity calculation

#### 3.1 Indirect Velocity Measurement

The accuracy of the system to measure flow velocity was also tested by measuring the wind tunnel velocity with the help of drag sensor with the theory of impact of fluid on a surface as in Figure 12 and comparing the results with measurements taken with the help of Pitot tube and differential manometer. The method also showed satisfactory results

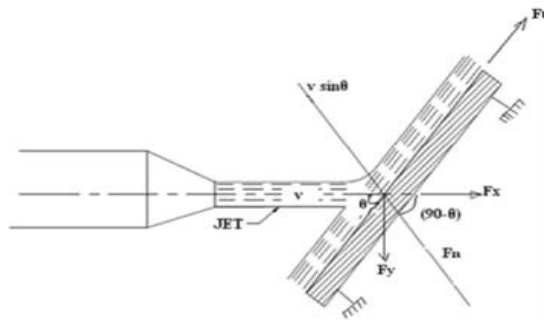


Figure 12. Force exerted by a jet on an inclined flat plate[6]

$a$  = area of cross section of the jet or the projected area of the wing parallel to flow  
 $v$  = velocity of the jet in direction of  $x$   
 $\theta$  = angle between jet and the plane  
 mass of the water striking the wing per sec =  $\rho av$   
 plate was assumed smooth and if it is assumed that there is no loss of energy due to the impact of the jet, then the jet will move over the plate after striking with a velocity equal to initial velocity  $v$   
 $F_n = \rho av[v \sin \theta - 0] = \rho av^2 \sin \theta$   
 $F_x = \rho av^2 (\sin \theta)^2$  (along the direction of the flow)  
 $F_y = \rho av^2 \sin \theta \cos \theta$  (perpendicular to flow)  
 $v = \sqrt{\frac{F_y}{\rho a \sin \theta \cos \theta}}$

Table - 2: Differential manometer velocity vs. experimental velocity

Velocity by differential manometer (m/s)	Experimental Velocity (m/s)
11	10
12	10.5
14	12.2
17	15.5
18	16
21	19.3
24	23

Following points were inferred from the data and experiment observation:

- There is an overall error of -9.52% in velocity measured by the system
- The error was possibly caused by linkage friction, uneven force distribution on sensor and inaccuracy in measuring strip lengths for torque balancing
- The system can be successfully used for measuring wind tunnel velocity if - 9.52% error

### 3.2 Experimental Data and Comparison with Literature

The airfoil NACA 4209 was mounted and the data's were recorded at various angle of attack and at velocities 11m/s, 12m/s, 14m/s. Further higher velocities were not experimented at because of safety reasons of the wind tunnel. Experimental datas were compared with datas from airfoil tools[1].

The formula used to measure error is Percentage Error = (Experimental value - Theoretical value)/Theoretical value

#### 6.2.1 Reynolds Number Calculation

The Reynolds number is an important dimensionless number required for lift and drag coefficients . It is the ratio of inertial forces to viscous forces and describes if a flow is laminar or turbulent. Airfoils or any other bodies at the same Reynolds number will have the same flow characteristics.

Reynolds number for an airfoil is calculated as:

$$Re = \frac{\rho v l}{\mu}$$

Where  $\mu$ = viscosity of air , $v$  = speed of air in wind tunnel,  $\rho$  = density of air and  $l$  = chord length of the airfoil

#### 3.2.2 Test 1

Table - 3: Test 1 specifications

Velocity	11m/s
Chord width	.395 m
Kinematic viscosity	1.511x 10 <sup>-5</sup> m <sup>2</sup> /s
Reynolds Number	287,539

##### 3.2.2.1 Lift Coefficient Analysis:

The following lift force data's were obtained at various angle of attacks:

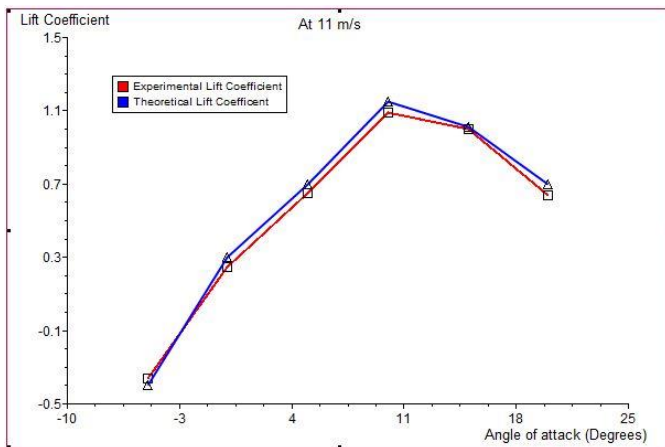
Table - 4: Test 1 Lift experiment result

Angle of attack( $\theta$ ) in degrees	Lift force (N)	Experimental Lift coefficient	Literature Lift coefficient
-5	-2.4	-.36	-.4
0	1.7	.25	.3
5	4.3	.65	.7
10	7.1	1.09	1.15
15	6.4	1	1.01
20	4	.64	.7

The following graph is obtained when lift coefficients are plotted against angle of attack:

### 3.2.3 Test 2

Table - 6: Test 2 specifications



Velocity	12 m/s
Chord Width	.395 m
Kinematic Viscosity	$1.511 \times 10^{-5} \text{ m}^2/\text{s}$
Reynolds Number	313,679

Figure 13. Test 1 Lift coefficient vs. Angle Of Attack

#### 3.2.3.1 Lift Coefficient Analysis:

#### 3.2.2.2 Drag Coefficient Analysis:

The following lift force data's were obtained at various angle of attacks:

The following drag force data's were obtained at various angle of attacks:

Table - 7: Test 2 Lift experiment result

Table - 5: Test 1 Drag experiment result

Angle of attack( $\theta$ ) in degrees	Lift force (N)	Experimental Lift coefficient	Literature Lift coefficient
-5	-2.8	-.35	-.4
0	2.3	.29	.3
5	6.7	.858	.9
10	8.6	1.11	1.19
15	8	1.057	1.1
20	4	.543	.6

Angle of attack( $\theta$ ) in degrees	Drag force (N)	Experimental Drag coefficient	Literature Drag coefficient
-10	1.1	.167	.115
-5	.39	.059	.045
0	.2	.03	.015
5	.32	.048	.019
10	.5	.075	.039
15	1.4	.212	.119

The following graph in Figure 15 is obtained when lift coefficients are plotted against angle of attack:

The following graph in Figure 14 is obtained when drag coefficients are plotted against angle of attack:

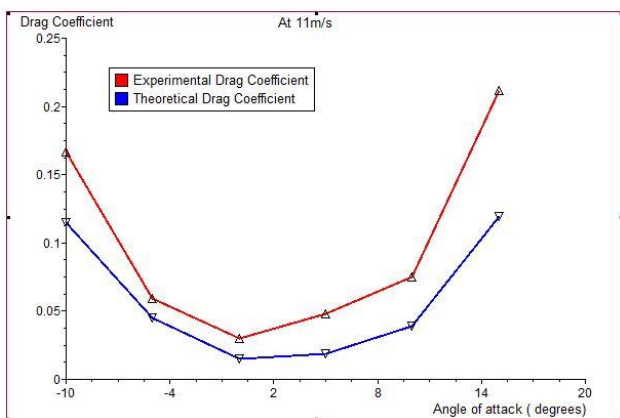
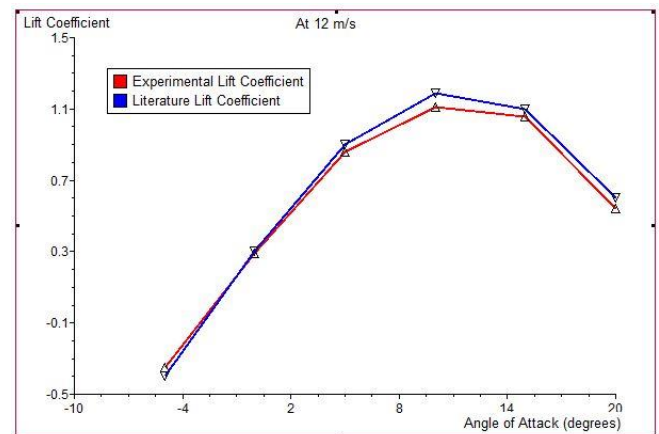


Figure 15. Test 2 Coefficient of lift vs. angle of attack

Figure 14. Test 1 Drag coefficient vs angle of attack

#### 3.2.3.2 Drag Coefficient Analysis:

The following drag force data's were obtained at various angle of attacks:

**Table - 8:** Test 2 Drag experiment results

Angle of attack( $\theta$ ) in degrees	Drag force (N)	Experimental Drag coefficient	Literature Drag coefficient
-10	1.3	.165	.105
-5	.5	.063	.05
0	.2	.025	.01
5	.41	.052	.015
10	.42	.063	.03
15	1.4	.178	.15

The following graph in Figure 16 is obtained when drag coefficients are plotted against angle of attack:

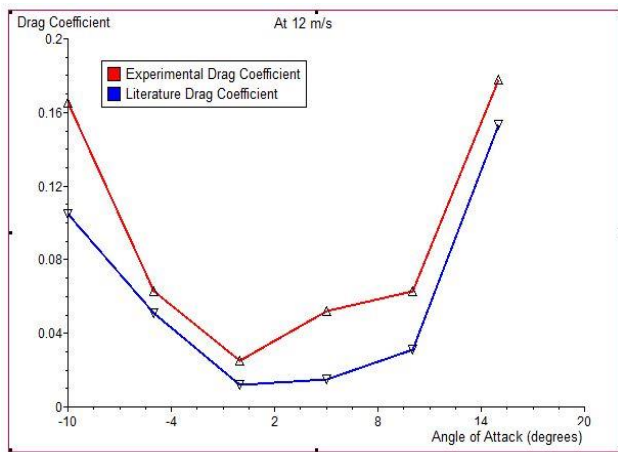


**Figure 16.** Test 2 drag coefficient vs angle of attack

### 3.2.4 Test 3

**Table - 9:** Test 3 specifications:

Velocity	14 m/s
Chord Width	.395 m
Kinematic Viscosity	$1.511 \times 10^{-5} \text{ m}^2/\text{s}$
Reynolds Number	365,959

#### 3.2.4.1 Lift Coefficient Analysis:

The following lift force data's were obtained at various angle of attacks:

**Table - 10:** Test 3 Lift experiment results

Angle of attack ( $\theta$ ) in degrees	Lift force (N)	Experimental Lift coefficient	Literature Lift coefficient
-5	-3.8	-.351	-.39
0	3.5	.328	.35
5	9.7	.914	.95
10	13.2	1.25	1.3

15	12.5	1.21	1.25
20	8.8	.879	.9

The following graph in Figure 17 is obtained when lift coefficients are plotted against angle of attack

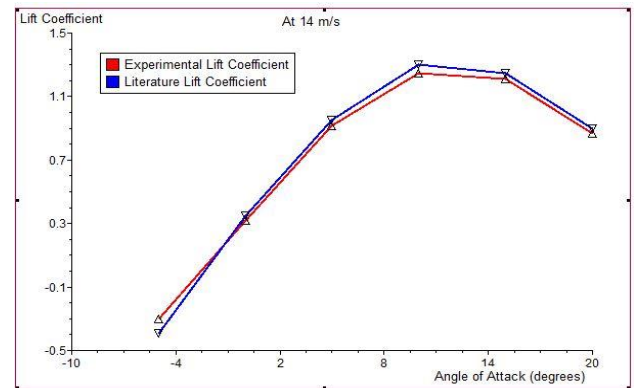


**Figure 17.** Test 3 lift coefficient vs. angle of attack

#### 3.2.4.2 Drag Coefficient Analysis:

The following drag force data's were obtained at various angle of attacks:

**Table - 11:** Test 3 Drag experiment results

Angle of attack( $\theta$ ) in degrees	Lift force (N)	Experimental Drag coefficient	Literature Drag coefficient
-10	1.3	.12	.1
-5	.5	.046	.03
0	.3	.028	.01
5	.25	.023	.012
10	.4	.037	.02
15	1.4	.131	.08

The following graph in Figure 18 is obtained when drag coefficients are plotted against angle of attack:

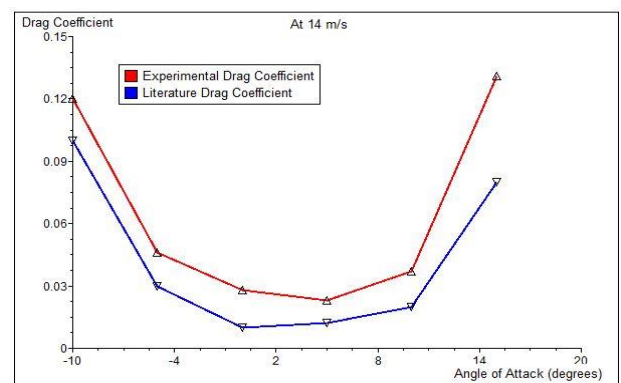


**Figure 18.** Test 3 drag coefficient vs. angle of attack

#### 4. Results And Discussions

Experiments were done at velocities 11m/s, 12m/s and 14m/s at various angle of attack following results were obtained:

- i. Vibrations were observed in the system which resulted in fluctuations in output that made inaccurate observations in small force ranges
- ii. Visible small bending were seen in the aluminum strips which suggested that stiffer materials would be better.
- iii. An overall error of 83.86% was inferred in coefficient of drag
- iv. An overall error of -6.56% was inferred in coefficient of lift.
- v. The large error in drag was due to concentration of drag forces across a narrow force range of 0 to .1 Newton and fluctuations which made gathering of drag data difficult.
- vi. The small error in lift coefficient was due to wide lift force distribution which ranged from 2 to 8 Newtons which made it possible to fix a mean position of fluctuation and thus analysable

This doesn't mean that the drag system is a failure; it means that it will be as accurate as the lift system in the force range experienced by the lift sensor; it also means that the drag system will be accurate when the airfoil has a large surface area or high wind tunnel velocities resulting in large drag forces. So the observations made it clear that the system can accurately measure forces with 93.4% accuracy provided forces are large. The indirect wind tunnel velocity measurement was also a success with 90.84% accuracy

#### 5. Conclusion

An error of 83.86% was inferred in coefficient of drag and -6.56% in coefficient of lift. The large error in drag was due to concentration of drag forces across a narrow force range of 0 to .1 Newtons and fluctuations which made it difficult to fix a mean position. The small error in lift coefficient was due to wide lift force distribution which ranged from 2 to 8 Newtons which were easily observable. It means that the drag system will be as accurate as the lift system in the force range experienced by the lift sensor. Overall, error in both the lift and drag forces should not fluctuate more than +/- 7% in large force ranges.

The cost of the setup did not exceed \$ 160. With the same design and few additional expenses the friction in linkage system, uniform pressure distribution in sensors, proper force distribution could be improved which will decrease the errors. The diagrams and equations presented in this paper will allow institutions and students to build this relatively low cost design for student projects and other

educational purposes with accuracy up to 93% to study the beautiful phenomenons of Fluid Dynamics.

#### 6. Acknowledgement

It is my privilege to express my sincerest regards to Professor (Dr.) Adnan Qayoum for his valuable guidance, encouragement, whole-hearted cooperation and constructive criticism

I deeply express my sincere thanks to the Head of Department of Mechanical Engineering (Dr) Prof. G.A Harmain and Professor (Dr.) Adnan Qayoum for encouraging and allowing me to carry out experiments in Fluid Mechanics Lab at NIT Srinagar

I also take this opportunity to pay my respects and love to my parents and all other family members and friends especially Shushil Kumar, Manish Meena and Mohd. Ikram for their love and encouragement.

#### 7. References

- [1] <http://airfoiltools.com/>
- [2] Frank M. White. Fluid Mechanics 7<sup>th</sup> edn University of Rhode Island. Publication company: Mc Graw Hill, 2010
- [3] Yunus A. Cengel, John M. Cimbala. Fluid Mechanics Fundamentals and Applications 1<sup>st</sup> edn  
Publication Company: Mc Graw Hill, 2004
- [4] <https://www.tekscan.com/products-solutions/force-sensors/a201>
- [5] <https://www.arduino.cc/en/main/arduinoBoardUno>
- [6] Dr. P.N. Modi and Dr. M. Sethi. Hydraulics and Fluid Mechanics including Hydraulics Mechanics 14<sup>th</sup> edn .  
Publication: Standard Bookhouse, 2009 .